Variation of Enhancement Factors and Relaxation Times at the Various Sites in Ordered Fe-Si Alloys

M. B. Stearns and J. F. Ullrich
Scientific Research Staff, Ford Motor Company, Dearborn, Michigan 48121
(Received 21 May 1971)

Pulsed NMR techniques have been used to measure the enhancement factors and longitudinal and transverse relaxation times in ordered Fe-Si alloys. The maximum enhancement factors of the alloys are large, becoming in some cases as large as seven times that in pure Fe. Both the behavior of the enhancement factors and relaxation times are well described by the drumhead model of domain walls. Using this model an expression is derived for the enhancement factor. Whereas in pure Fe the damping due to eddy currents appears to determine the behavior of the enhancement factor, for these alloys the terms due to damping and stiffness of the wall appear to be of comparable importance. For the alloy series, the maximum enhancement factor is seen to vary in much the same manner as the initial permeability. The relaxation rates for these alloys are usually slightly larger than those of pure Fe. Thus the relaxation mechanism appears to be via emission or absorption of a single magnon. For a given alloy the relaxation time from site to site may vary as much as a factor of 3 to 4. This may reflect resonance or virtual magnon levels in the spin-wave spectrum.

I. INTRODUCTION

Many properties of the ordered Fe-Se system have been studied extensively. It appears to be an ideal system in which to study many phenomena. Using pulsed NMR techniques we have measured the enhancement factors and longitudinal, T_1, and transverse, T_2, relaxation times at the various Fe and Si sites. The frequency spectra of the internal fields had been measured by Mössbauer[1] and NMR techniques.[2-4] The present experiments are performed with no external field so only nuclei in the domain walls are seen. The results indicate that the domain walls are well described by the drumhead model.[5] Using this model we derive an expression for the enhancement factor including wall mass, damping, and stiffness terms. The drumhead model automatically gives an expression for the natural frequency of vibration of the domain walls. Whereas in pure Fe the magnitude and behavior of the enhancement factor appears to be determined by the damping term due mainly to eddy currents, in the ordered alloys the stiffness of the walls appears to be equally important in determining the motion of the walls.

The relaxation times are comparable in magnitude and behavior with those for pure Fe.[6] Thus for these alloys the relaxation mechanism also appears to be due to emission or absorption of a single bulk magnon. In a given alloy the relaxation times at the various sites may vary by as much as a factor of 3 or 4; this may reflect resonance or virtual magnon states in the spin-wave spectrum.

II. EXPERIMENTAL PROCEDURE

Samples of ordered alloys varying from 14.7 to 25 at.% Si (all components will be given in at.%) were made in the following manner. A 5-lb ingot of 99.9% purity Fe and high-purity Si was prepared in an induction vacuum furnace. The ingot was then machined to obtain fine turnings which were then ground down to pass through a 74-μ sieve. These powders were next heat treated in an argon atmosphere. They were first heated to 850 °C for about 4 h, then slowly cooled to 400 °C and held there overnight. The furnace was then turned off and allowed to cool to room temperature; this took about 8 h. As is evident from the experimental results[4] the samples were essentially perfectly ordered.

The pulsed NMR apparatus was essentially the same as that described previously.[5] The measurements were made at 1.2 and 4.2 °K.

The enhancement-factor curves were taken in either of two ways: (i) by measuring the echo height as a function of the rf field B_1 with the pulse lengths τ_1 and τ_2 held constant or (ii) by varying τ_1 and τ_2 with B_1 held fixed. Both ways gave equivalent results. The ratio of the pulse lengths used was always kept at $\tau_2/\tau_1 = 2.1$, which gives the maximum echo height for a narrow-line case, i.e., $\gamma_n \epsilon_0 B_1 > \Gamma$, where γ_n is the nuclear gyromagnetic ratio, ϵ_0 the maximum enhancement factor at the center of a 90° wall, and Γ is the linewidth. The B_1 values were obtained by measuring the voltage induced in a single turn of wire around the cylindrical powdered samples. B_1 thus contains the mean permeability of the sample under the operating conditions. The enhancement-factor curves for these ordered alloys agreed very well with the drumhead model of a domain wall[5] where the echo height at the resonance frequency ω_n is given by

$$\mathcal{E}(\omega_n) \simeq \int_0^1 \int_0^1 \int_0^\infty \int_0^\pi \epsilon \sin\alpha_1 \sin^2(\tfrac{1}{2}\alpha_2) \cos\eta$$

$$\times p(h) r \sin\eta \, d\eta \, dx \, dr \, dh \,, \quad (1)$$

where $\epsilon = \epsilon_0 \operatorname{sech} x (1 - r^2) h$, α_n is the turning angle due to the nth pulse $\gamma_n \epsilon B_1 \tau_n$, x is the perpendicular distance (in characteristic wall-width units) from the center plane of the wall, r is the radial position of the nucleus in the drumhead measured in units of the drumhead radius r_0, h is the maximum displacement at the center of the drumhead measured relative to the maximum displacement of the largest-area drumhead, η is the angle between the rf magnetic field and the magnetization in the domains adjacent to the domain wall, and $p(h)$ is the probability distribution of the h's (see Ref. 5). Or, in the more convenient form for calculation, we have

$$\mathcal{E}(\omega_n) \simeq \epsilon_0 \int_0^\infty \int_0^1 \sin\alpha_1 \sin^2(\tfrac{1}{2}\alpha_2) z \operatorname{sech} x \times \ln^2(1/z) \, dz \, dx \,, \quad (2)$$

where $z = (1 - r^2) h \cos\eta$ (see the Appendix in Ref. 5) and $hp(h) = Ap(A)$ is taken equal to a constant. A is a domain-wall area and $p(A)$ the probability distribution of the A's. Figure 1 shows a typical enhancement-factor curve. The solid line is the variation given by Eq. (2) for $\epsilon_0 = 30\,000$. The ϵ_0 value is obtained by adjusting the curve of Eq. (2) to fit the experimental data by varying the maximum turning angle given by $\alpha_1^0 = \gamma_n \epsilon_0 B_1 \tau_1$. Since B_1 and τ_1 are known, only ϵ_0 is unknown. The enhancement factor can be determined to about 5–10%. Most of the uncertainty arises from the measurements of B_1 and the pulse lengths.

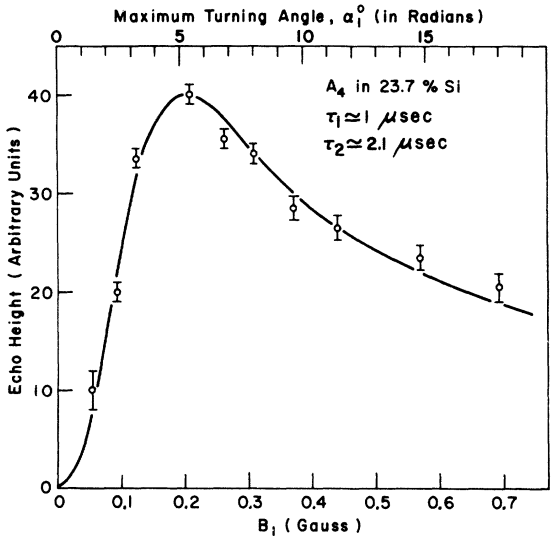

FIG. 1. Typical enhancement-factor curve for the A_4 line in the 23.7% Si alloy. The solid curve is that derived from the drumhead model of domain walls with the maximum enhancement factor $\epsilon_0 \simeq 30\,000$. (Si concentration given in at.%.)

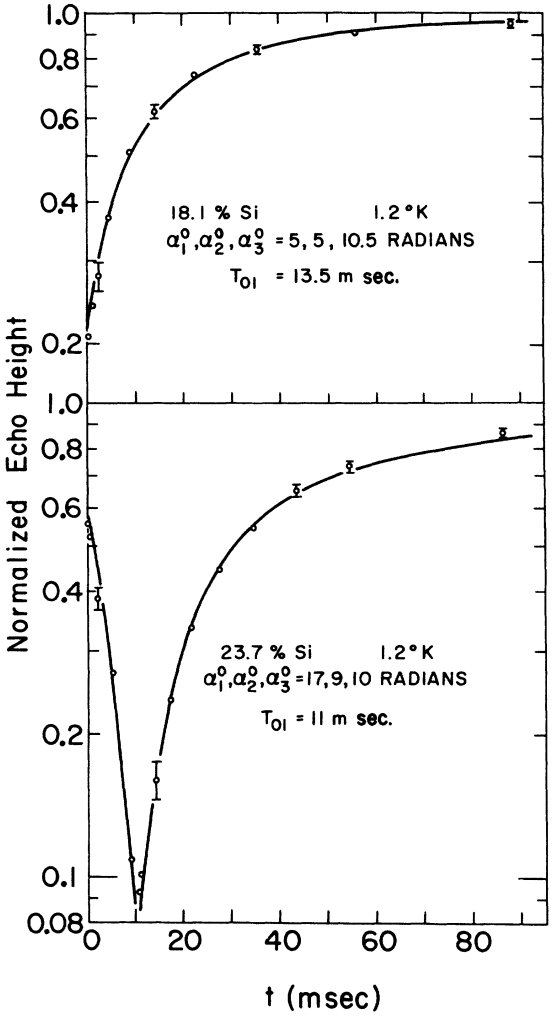

FIG. 2. Typical curves for determining the longitudinal relaxation times. Both curves are for D sites. The solid line is calculated using the drumhead model to describe the wall motion, as given by Eq. (3). (Si concentration given in at.%.)

The T_1 values were obtained by measuring the nuclear magnetization at a time t after a pulse τ_0. This was accomplished by measuring the echo height due to a pair of pulses, τ_1 and τ_2. Using the drumhead model and assuming the relaxation occurs via the emission or absorption of a single magnon[6] (the spin-wave spectrum is assumed to extend to zero energy because of the demagnetizing fields), the echo height at the resonance frequency is given by[6]

$$\mathcal{E}(t) \sim \epsilon_0 \int_0^\infty \int_0^1 \sin\alpha_1 \sin^2(\tfrac{1}{2}\alpha_2) \left[1 - (1 - \cos\alpha_0)\right] \times e^{-t(\operatorname{sech}^2 x)/T_{01}} z \operatorname{sech} x \ln^2(1/z) \, dz \, dx \,, \quad (3)$$

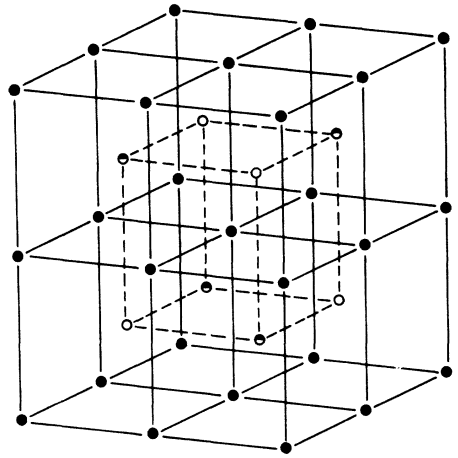

FIG. 3. Structure of ordered Fe_3Si.

where T_{01} is the smallest relaxation time at the center plane of the wall. T_{01} is the only unknown parameter and can be obtained by fitting the measured data with Eq. (3). Some typical relaxation curves are shown in Fig. 2. The solid lines are given by Eq. (3) with the values of T_{01} listed in Fig. 2. The measured curves fit the drumhead model very well. The data were usually taken with α_0^0, α_1^0, and α_2^0 equal to 5, 5, and 10.5 rad since this combination has a quite sensitive shape. To assure complete recovery of the equilibrium magnetization the time between each series of three pulses was 1 sec. The time between τ_1 and τ_2 was 100 μsec, which is much shorter than the minimum transverse relaxation time. The free-induction decay time of the alloys was between 2 and 5 μsec, corresponding to linewidths of 100–200 kHz.

The transverse relaxation time was measured by the usual method of measuring the echo height as a function of the time t between two pulses, τ_1 and τ_2. Again using the drumhead model for the wall motion and assuming that the relaxation occurs via the emission or absorption of a single magnon, the echo height at resonance is given by[6]

$$\mathcal{E}(t) \sim \epsilon_0 \int_0^\infty \int_0^1 \sin\alpha_1 \sin^2(\tfrac{1}{2}\alpha_2)\, e^{-2t\,(\mathrm{sech}^2 x)\,/\,T_{02}} \times z\,\mathrm{sech}x \ln^2(1/z)\,dz\,dx\,, \quad (4)$$

where T_{02} is the smallest relaxation time at the center of the wall and is the only unknown parameter in Eq. (4). T_{02} is obtained by fitting Eq. (4) to the measured transverse relaxation curves. The agreement with the drumhead model is again excellent. The data were usually taken with α_1^0 and α_2^0 equal to 5 and 10.5 rad. See Fig. 5 of Ref. 6 for typical transverse relaxation curves. Again the repetition rate used was one echo sequence per second.

III. EXPERIMENTAL RESULTS AND DISCUSSION

The structure of ordered Fe_3Si is shown in Fig. 3. There exist three different type sites: D sites which have 8 nearest-neighbor (NN) Fe atoms, Si sites, and A sites which in Fe_3Si have 4 NN Fe atoms and NN Si atoms. As Fe is added to Fe_3Si the excess Fe atoms go randomly into the Si sites.[1] We then get different A_n-type sites, where n denotes the number of NN Fe atoms. We see A_4-, A_5-, and A_6-type sites depending on the Si content (see Ref. 4 for a more complete discussion of these sites).

A. Enhancement Factors

The enhancement factors were essentially the same at 1.2 and 4.2 °K. They are listed in Table I. The enhancement factor is sensitive to impurities and other structure-sensitive properties (like strains, shape anisotropy, crystallite dimensions, etc.). It is also dependent upon the domain-wall size, which is partially determined by the structure-sensitive properties. Since these properties are dependent upon the impurities, heat treatment, etc., we have separated and listed as a matched set those alloys which were made up and processed at the same time (see Table I). The unmatched 24.9, 22.95, and 21.95% alloys were made, ground, and heat treated at different times. The 18.4% Si alloy was part of the matched set but intentionally had 0.07% Hf added. This is known to reduce the grain size in these ordered alloys and this was confirmed by taking metallographic photographs of the grain sizes. The heat-treated ingot of the 18.1% alloy (no Hf) has grain sizes of roughly 10 times the grain size of the 18.4% alloy (0.07% Hf). We also looked at the domains by the Bitter pattern techniques. The difference in domain size in the two alloys was not as great as the grain-size difference.

TABLE I. Maximum enhancement-factor values ϵ_0. $R(A_4/\mathrm{Si}) = 6.3 \pm 0.5$.

			Matched set		
at. % Si	23.7	21.6	19.8	18.1	14.7
D	27 500	42 000	42 000	39 000	52 000
A_4	21 000	21 000	26 000	30 000	
Si	3 500	4 200			
			Unmatched samples		
at. % Si	24.9	22.95	21.95	18.4(Hf)	
D	11 000	17 000	14 000	18 000	
A_4	9 600	13 000	12 000		
Si	1 400	2 000	1 600		

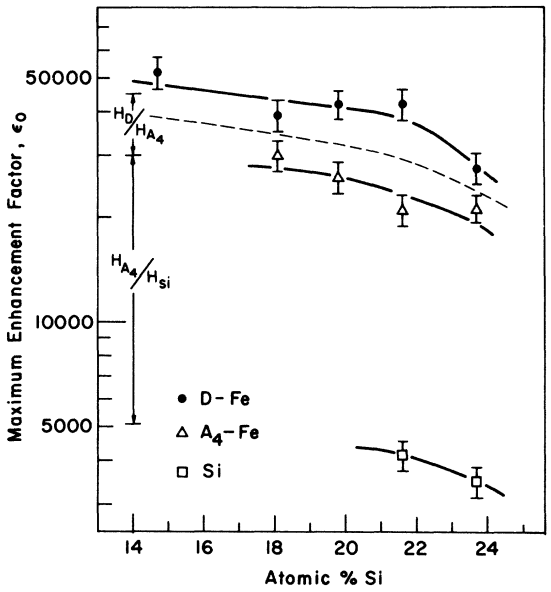

FIG. 4. Maximum enhancement factors of the matched set alloys. The value of ϵ_0 is seen to be proportional to the internal field and is seen to decrease with increasing Si content.

It appeared to be only about a factor of 2 or 3 larger in the no-Hf alloy. We see from Table I that the (no-Hf) alloy had a maximum enhancement factor for the D sites of $\epsilon_0 \sim 39\,000$ while the 18.4% (Hf) alloy had $\epsilon_0 \sim 18\,000$. The enhancement factors were, of course, measured in the small powdered crystallites, not in the ingots which were examined. This suggests that the stiffness term may dominate over the viscosity term in these alloys (see discussion below).

Thus, for further comparisons we will consider only the matched-set enhancement factors which are shown in Fig. 4. We see two trends in these data: First, the enhancement factors at the A_4, D, and Si sites are very nearly proportional to the internal fields. The internal field ratios are shown on the left-hand side of Fig. 4. (For a complete list of the internal fields, or resonance frequencies, see Ref. 4.) The second observable trend is that ϵ_0 for any type site seems to decrease with increasing Si content.

Let us now calculate the wall-enhancement factor for domain walls which behave like circular membranes with fixed perimeters [as shown in Fig. 5(a)]. Using a procedure parallel to that of Refs. 7 and 8 we write the equation of motion for small displacement ξ of the drumhead-type domain walls during the time when the rf field is on. It is

$$m_w \frac{\partial^2 \xi}{\partial t^2} + \beta \frac{\partial \xi}{\partial t} - \alpha \left(\frac{\partial^2 \xi}{\partial r^2} + \frac{1}{r} \frac{\partial \xi}{\partial r} \right) = 2 M_s H_1(t) J_0(kr) , \tag{5}$$

where m_w is the wall mass per unit area, β is the damping constant, α is the stiffness of the drumhead-type wall, M_s is the saturation magnetization, $H_1(t)$ is the oscillating rf field ($= H_1 e^{i\omega t}$), and r is the radial position in the membrane of radius r_0. The assumption that the domain walls look like a circular membrane pinned at its circumference gives rise to the radial dependence of a zeroth-order Bessel function $J_0(kr)$ where

$$k = (m_w/\alpha)^{1/2} \omega_0 .$$

With no rf driving force the condition that the wall be stationary at its perimeter, i.e., $J_0(ka) = 0$, leads to an expression for the natural frequency of the wall:

$$\omega_0 = \frac{2.4}{r_0} \left(\frac{\alpha}{m_w} \right)^{1/2} . \tag{6}$$

For a periodic driving field, the wall displacement is given by

$$\xi = \xi_0 J_0(kr) e^{i\omega_n t} , \tag{7}$$

where the maximum displacement is

$$|\xi_0| = \frac{2 M_s H_1}{m_w [(\omega_0^2 - \omega_n^2)^2 + (\beta/m_w)^2 \omega_n^2]^{1/2}} . \tag{8}$$

When the rf field tilts the atomic spin through an angle θ, for small θ, the nuclear spin sees an effective rf field B_n of [see Fig. 5(b)]

$$B_n = \theta H_n , \tag{9}$$

where H_n is the internal field at the nucleus. In the domain wall the spin directions vary with position x in the wall, and this variation was evaluated by Kittel and Galt (KG).[7] In particular the quantity $\Delta\theta/\Delta x$ is evaluated for a 90° wall and is given by

$$\frac{\Delta\theta}{\Delta x} = \frac{1}{2\delta} \operatorname{sech}\left(\frac{x}{\delta} \right) , \tag{10}$$

where δ is the characteristic wall width and is about $\frac{1}{4}$ the thickness of a 180° wall. It is given by

$$\delta = (A/K)^{1/2} ,$$

where A and K are the exchange and crystalline anisotropy constants. Now by small displacement

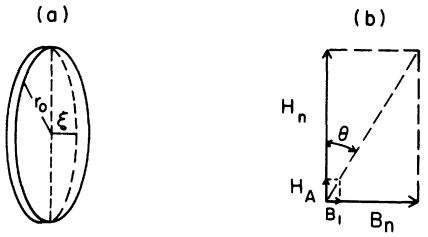

FIG. 5. (a) Drumhead model for domain wall. (b) Vector diagram of atomic (H_A, B_1) and nuclear (H_n, B_n) magnetic fields.

in deriving Eq. (5) we mean specifically that $\xi \ll 4\delta$. Under this condition the angle of turn of the atomic spin at a given position x in the domain wall for a displacement ξ is given by $\theta = (\Delta\theta/\Delta x)\xi$. Thus in the wall a displacement ξ causes the nuclear spin to see an effective field B_n of

$$B_n = (\Delta\theta/\Delta x)\xi H_n \ . \qquad (9')$$

Substituting Eqs. (8) and (10) in Eq. (9'), the rf field seen by the nucleus is

$$B_n = -\frac{M_s H_n \operatorname{sech}(x/\delta) J_0(kr)}{\delta m_w[(\omega_0^2 - \omega_n^2)^2 + (\beta/m_w)^2\omega_n^2]^{1/2}} H_1 . \qquad (11)$$

We previously defined the enhancement factor[5] as the ratio of B_n/B_1, since B_1 in the samples is easily measurable and we did not want to determine the permeability μ for each sample. Furthermore, since μ depends upon the packing fraction, it is sometimes a rather arbitrary parameter. Other authors, however, have defined ϵ as the ratio of B_n/H_1 and care must therefore be taken in comparing different authors' enhancement factors.[8] Thus the enhancement factor ϵ $(= B_n/B_1)$ is given by

$$\epsilon = \frac{M_s H_n \operatorname{sech}(x/\delta) J_0(kr)}{\mu\delta m_w[(\omega_0^2 - \omega_n^2)^2 + (\beta/m_w)^2\omega_n^2]^{1/2}} . \qquad (12)$$

In Refs. 5 and 6 we used the approximation $J_0 \simeq 1 - (r/r_0)^2$.

Let us now consider the sizes of the various terms in the denominator. For Fe or the Fe-Si alloys we expect ω_0 to be much larger than the nuclear resonance frequencies (30–50 MHz). The stiffness α of the drumhead wall depends on the detailed mechanism of the wall movement, but the minimum value this quantity could have is the wall energy per unit area σ_w as determined from only the anisotropy and exchange energies. KG[7] have derived this wall energy and find

$$\sigma_w = 2(KA)^{1/2} .$$

They also obtain the wall mass as

$$m_w = (1/4\pi\gamma^2)(K/A)^{1/2} ,$$

where γ is the electron gyromagnetic ratio. We thus obtain

$$\omega_0 \geq 2.4(8\pi\gamma^2 A)^{1/2} r_0 . \qquad (13)$$

Using the values listed in Table II, $\omega_0 \geq 3.7\times10^9/r_0$ rad/sec for r_0 given in microns.

From Eq. (8) if ω_0 dominates we get the following.

Case I: $\omega_0 \gg \omega_n$, (β/m_w). We have

$$|\xi_0| \leq \frac{2M_s H_1}{m_w\omega_0^2} = \frac{2M_s H_1 r_0^2}{(2.4)^2\sigma_w} .$$

Using values in Table II for Fe we get $\xi_0 \sim 280 H_1 r_0^2$. Thus for $H_1 \sim 0.5$ G, $r_0 = 1$ μ we get

$$\xi_0 \leq 140 \text{ Å (Fe)} .$$

TABLE II. Values for various parameters of Fe.

	Fe	$Fe_3Si(D)$
$A(=2JS^2/a)$	2×10^{-6} erg/cm	1.5×10^{-6} erg/cm
M_s	1700 kG	1000 kG
H_n(Fe)	340 kG	
K(4.2 °K)	5.2×10^5 erg/cm^3	
σ_w(4.2 °K)	2.1 erg/cm^2	
m_w(4.2 °K)	10^{-10} g/cm^2	
γ	1.76×10^7 rad/sec G	
$\delta[=(A/K)^{1/2}]$	200 Å	

We obtain from Eq. (12) that the maximum enhancement factor is

$$\epsilon_0 \leq \frac{M_s H_n}{\mu\delta m_w\omega_0^2} = \frac{H_n r_0^2 M_s}{2\times(2.4)^2\mu A} . \qquad (14)$$

For Fe, μ was measured to be about 3; thus using the values in Table II we get $\epsilon_0 \leq 8\times10^{12} r_0^2$. Thus for $r_0 \sim 1$ μ we get $\epsilon_0 \leq 8\times10^4$ (Fe). This was the case implicitly assumed in Ref. 5. We see that the maximum displacement $\xi_0 (\equiv h)$ is proportional to the area of the drumhead. Thus the probability distribution of h, $p(h)$, is proportional to $p(A)$, and $Ap(A)$ was assumed to be a constant in taking the average over the drumhead sizes. We measured an $\epsilon_0 \sim 6000$ for Fe at 4.2 °K so both ξ_0 and ϵ_0 seem too large for reasonable values of r_0.

However for the Fe-Si ordered alloys, Eq. (14) gives a value of $\epsilon_0 \lesssim 60000$ for $r_0 \sim 1$ μ, in satisfactory agreement with the observed D-site value of $\epsilon_0 \sim 40000$.

Case II: $\beta/m_w \gg \omega_n$, ω_0. Now let us estimate the size of the viscosity term. In ferromagnetic metals which are good conductors the major energy loss is likely to be due to the eddy-current damping (with hysterisis losses being comparable in some cases). We derive the braking (or demagnetizing) field due to eddy currents similarly to Stewart,[9] but we assume that the domain wall is a disk of radius r_0 (see Fig. 6) which is fixed at its perimeter. Then the change in magnetic moment for a displacement ξ at the center is $2M_s\Delta V$, where $\Delta V = \frac{1}{2}\pi r_0^2\xi$. The time rate of change of moment is thus

$$\frac{\delta M}{\delta t} = \pi M_s r_0^2 v ,$$

where $v = \omega\xi$. The rate of change of flux through an annulus at distance r and angle θ is then

$$\frac{\delta\varphi_r}{\delta t} = \frac{2}{r^3}\frac{\delta M}{\delta t}\int_0^\theta \cos\theta\, 2\pi r \sin\theta\, r\, d\theta = \frac{2\pi}{r}\frac{\delta M}{\delta t}\sin^2\theta .$$

A voltage of $2\pi r\sin\theta\,\rho\delta i$ will develop around the annulus (where ρ is the resistivity and δi is the current). Thus

$$2\pi r \sin\theta\, \rho \delta i = \frac{2\pi}{r}\frac{\delta M}{\delta t} \sin^2\theta\, r\, dr\, d\theta \ .$$

This gives a current of

$$\delta i = \frac{\delta M}{\delta t}\frac{\sin\theta}{\rho r}\, dr\, d\theta \ ,$$

flowing around the annulus. This then gives rise to the braking field at the wall of

$$\delta H_b = \frac{2\pi \sin^2\theta}{r}\, \delta i \ .$$

Integrating over all values of θ and r going from a lower limit to infinity we get

$$H_b = \frac{8\pi^2}{3}\frac{M_s r_0 v}{\rho} 10^{-9} \ , \tag{15}$$

where ρ is in Ω cm. We have taken r_0 as the lower limit of integration, as seems reasonable for a drumhead-type wall. Since this braking field gives rise to the damping term we set

$$\beta v = 2M_s H_b$$

and obtain

$$\beta = \tfrac{16}{3}\pi^2 \times 10^{-9} M_s^2 r_0/\rho \ . \tag{16}$$

When the damping term determines the amplitude of oscillation of the drumhead we should of course treat the whole problem in a self-consistent manner and consider the phases of the applied and braking field. However, we want only a rough estimate of β since many other approximations are made throughout the whole treatment. Let us estimate the frequency β/m_w for Fe at 4.2 °K. We obtain

$$\beta \simeq 0.15\, r_0/\rho \ \mathrm{g/cm^2\,sec}$$

or

$$\beta/m_w \simeq 1.5\times 10^9 r_0/\rho \ \mathrm{rad/sec} \ ,$$

where r_0 is in cm and ρ in Ω cm. In Fig. 7 we show $\omega_0^2 - \omega_n^2$ and $(\beta/m_w)\omega_n$ as functions of r_0 for

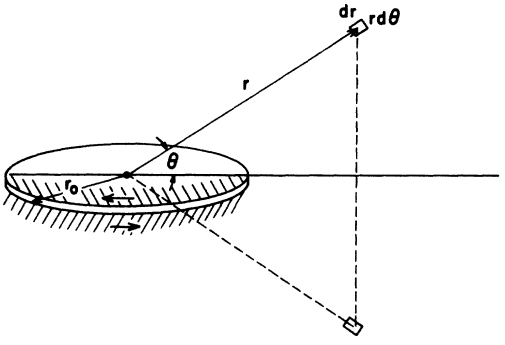

FIG. 6. Diagram for calculation of viscosity resulting from eddy currents assuming a drumhead-type domain wall.

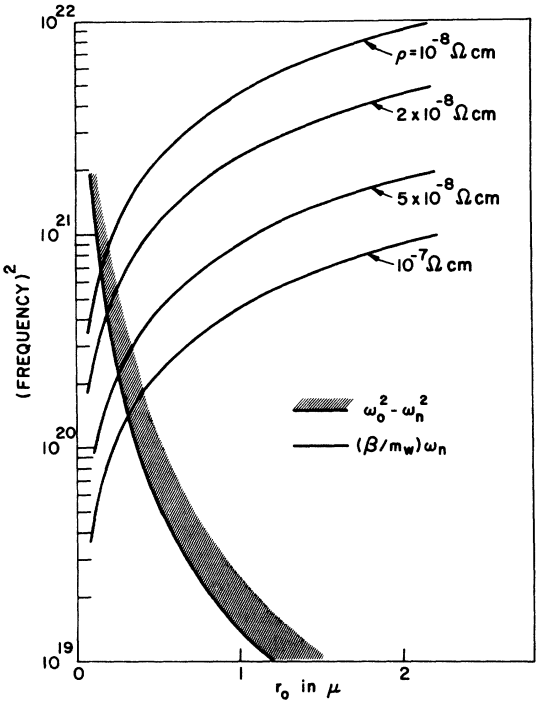

FIG. 7. Plot of terms in the denominator of Eq. (8) as a function of wall radius r_0 for various resistivities ρ [for ω_n (Fe and D sites) = 3×10^8 rad/sec]. For Fe at $r_0 \geq 0.3$–$0.5\ \mu$ the damping term begins to dominate.

different values of ρ [for ω_n(Fe) = 3×10^8 rad/sec]. It is very difficult to estimate the value of ρ in our samples since the skin depth is small (about a micron) and there are probably impurities in some of this layer. A reasonable guess is that ρ is in the range from 5×10^{-7} to 5×10^{-8} Ωcm. In that case we see from Fig. 7 that the damping term will dominate for r_0 of 0.3–0.5 μ or greater. If the damping term dominates we have from Eq. (8)

$$|\xi_0| \simeq \frac{2M_s H_1}{\beta\omega_n} = \frac{3\times10^9 H_1}{8\pi^2 M_s \omega_n}\frac{\rho}{r_0} \tag{17}$$

and

$$\epsilon_0 \simeq \frac{M_s H_n}{\mu\delta\beta\omega_n} = \frac{3\times10^9}{16\pi^2}\frac{H_n\rho}{\mu\delta\omega_n M_s r_0} \ . \tag{18}$$

For the Fe powdered samples[5] $\mu \simeq 3$, so we get $\epsilon_0 \simeq 2.1\times10^6\,\rho/r_0$. We measured ϵ_0 to be ~6000, thus for $r_0 \sim 1\ \mu$ we find $\rho \sim 3\times10^{-7}$ Ωcm. These are reasonable values; we expect r_0 to be $\frac{1}{2}\mu$ or greater and ρ to be around 5×10^{-7} Ωcm or less. This would indicate that indeed the damping term does dominate in pure Fe. In Ref. 5, ϵ_0 was observed to increase with temperature from ~6000 at 4.2 °K to ~19000 at 298 °K. According to Eq. (18) this increase is mainly due to an increase in ρ. (If r_0 increases with temperature due to unpinning of the wall at imperfections, this increase is

unlikely to be as rapid as the increase in ρ.) For $H_1 \sim 0.5$ G, $r_0 \sim 1$ μ, and $\rho \sim 3\times10^{-7}$ Ωcm, we find $\xi_0 \simeq 10$ Å. So ξ_0 is much smaller than the wall thickness of ~1000 Å.

In Fe_3Si we expect β to be less than β in Fe by about a factor of 10, and thus the ω_0 term may become comparable to the damping term. We would thus get an enhancement factor in the range of 60 000, which is in satisfactory agreement with those obtained for the D sites in the ordered alloys.

Notice from Eq. (17) that if the damping term dominates, the maximum displacement ξ_0 (or h) varies as $1/r_0$ rather than as r_0^2, as it did in the case where the stiffness term dominated. Thus setting $hp(h) = \text{const}$ is equivalent to taking $r_0 p(r_0) = \text{const}$ in contrast to taking $Ap(A) = \text{const}$ when ω_0 dominates (Case I). Either distribution is arbitrary and equally reasonable.

A question of interest is why, at zero applied field, do we never observe nuclei in the domain? The domain enhancement factor is given by

$$\epsilon_D = H_n/H_A ,$$

where the static anisotropy field H_A is equal to $2K/M_s$ (see Ref. 7). Thus we get

$$\epsilon_D \sim 600 ,$$

which is about a factor of 10 less than the ϵ_0 value observed at 4.2 °K for Fe or about a factor of 60 less than ϵ_0 for the ordered alloys. Another effect also decreases the apparent domain signal. This is the spread in resonance frequencies of the domain nuclei due to the variation in the demagnetizing fields from different-shaped particles; the wall nuclei are shielded from the demagnetizing fields.

In Fig. 8 we show that the enhancement factors of the matched set of ordered alloys decrease with increasing Si content (same as the dashed line of Fig. 4). We also show ρ/M_s as would be obtained for the variation of ϵ_0 if the damping term were dominant, see Eq. (18). The values of ρ are assumed to vary as the bulk material,[10] and the M_s values are taken from Matsumoto.[11] Also shown is the variation of ϵ_0 which would be obtained if the surface-tension term were dominant as in Eq. (14). The variation would then go as the ratio M_s/A (taken as manifest by the Curie-temperature varia-

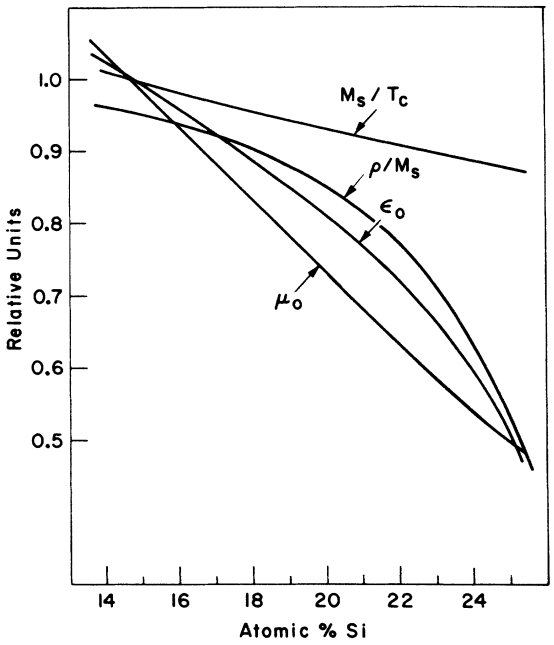

FIG. 8. Variation of maximum enhancement factor ϵ_0, ρ/M_s, M_s/T_c, and initial permeability μ_0 with Si content.

TABLE III. Minimum longitudinal (T_{01}) and transverse (T_{02}) relaxation times at the center of the wall.

	24.9		23.7		21.6		19.8		18.1		14.7	
	T_{01}	T_{02}	T_{01}	T_{02}	T_{01}	T_{02}	T_{01}	T_{02}	T_{01}	T_{02}		
						(4.2 °K)						
D	4 ± 1	8.5 ± 1	4.5 ± 0.5	5 ± 1	7 ± 2	5 ± 2		5 ± 1	2.5 ± 1		2.5 ± 0.5	
A_6										9 ± 2	2.5 ± 0.5	
A_5			7 ± 1	6 ± 2				8 ± 1	5.5 ± 1	5 ± 2	4.5 ± 1	
A_4	6 ± 1	12.5 ± 1	7 ± 1	9.5 ± 1								
Si	6 ± 2	4.5 ± 1	9 ± 1	4 ± 1								
Fe[a]	11 ± 1	11 ± 2										
						(1.2 °K)						
D	12 ± 1	23 ± 1	12 ± 1	14 ± 1	25 ± 3	20 ± 3	11 ± 2	9 ± 1	13.5 ± 1	9 ± 1	13 ± 1	13 ± 2
A_6							18 ± 2	8 ± 1	15 ± 2	10 ± 2	15 ± 2	11 ± 1
A_6			15 ± 2	15 ± 2	16 ± 2	17 ± 2	18 ± 2	19 ± 2	16 ± 2	19 ± 2	18 ± 2	18 ± 2
A_4	20 ± 1	26 ± 1	13 ± 2	26 ± 2	23 ± 2	17 ± 2	16 ± 2	26 ± 2	25 ± 2	23 ± 2		
Si	19 ± 1	6.5 ± 1	21 ± 2	9.5 ± 1	22 ± 2	11 ± 2						
Fe[a]	40 ± 5	33 ± 2										

[a]See Ref. 6.

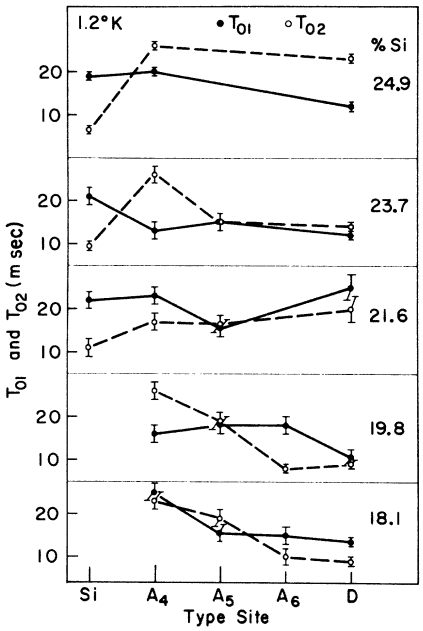

FIG. 9. Variation of minimum longitudinal (T_{01}) and transverse (T_{02}) relaxation times (at the center of the wall) for the different types of sites. (Si concentration given in at.%.)

tion). The values of T_c are from Fallot.[12] The variation of ϵ_0 is more rapid than M_s/T_c but is in fair agreement with the ρ/M_s variation. This would suggest that the damping term is important for these alloys. However, using the bulk resistivity values may not be appropriate; further, we have neglected any change in δ and r_0 with alloying. We saw earlier from the magnitude of ϵ_0 that ω_0^2 may be comparable to $(\beta/m_w)\omega_n$ in these alloys.

As shown in Fig. 4, the maximum enhancement factor appears to be proportional to H_n at the different sites. If the stiffness term were dominant according to Eq. (14) we have for a given alloy

$$\epsilon_0 \sim H_n/\mu \ .$$

Since $\mu \sim \omega_n^{-1/2}$, we have $\epsilon_0 \sim \omega_n^{3/2}$. On the other hand, if the damping term were dominant, according to Eq. (18) we have

$$\epsilon_0 \sim H_n/\mu\omega_n \sim \omega_n^{1/2} \ .$$

The observed variation of $\epsilon_0 \sim H_n$ (or ω_n for a given site) would indicate that we have an intermediate case in these alloys or that both terms are comparable.

Thus in pure Fe the viscosity term appears to be dominant and to determine the magnitude of the enhancement factor, while in the ordered alloys the increased resistivity and decreased saturation magnetization decrease the eddy currents, and therefore the viscosity term and the stiffness term appear to become of comparable importance.

Another quantity that is also dependent on the domain-wall motion and is thus likely to correlate with ϵ_0 is the initial permeability μ_0. The relative variation of μ_0 with Si content[11] is shown in Fig. 8 and indeed is seen to behave similarly to ϵ_0.

B. Relaxation Times

We list in Table III the fastest longitudinal (T_{01}) and transverse (T_{02}) relaxation times which occur at the center of the walls. The relaxation times are not noticeably dependent on structure-sensitive properties. We see that in general the 1.2 °K values are about three times longer than the 4.2 °K values, in agreement with the linear temperature dependence of the relaxation rates as found in pure Fe.[6] The relaxation times vary between being about half those obtained for pure Fe and being comparable to them. The longitudinal relaxation rates measured at the center of the domain wall for Fe[6] and Ni[13] are, respectively, about 300 and 30 times greater than the rates calculated assuming that the relaxation occurs through interaction with the itinerant electrons.[14] This and the fact that the relaxation rates vary as expected for coupling with the magnon field $[1/T_1 \sim (\mathrm{sech}^2 x)/T_{01}]$ lead us to propose that the relaxation occurs by emission or absorption of a single magnon[6] in Fe. The mechanism appears to be the same for the ordered alloys.

For the A and D sites of the nearly stoichiometric alloy (24.9% Si), the T_{02} relaxation times appear to be nearly twice as long as T_{01}. This is just the ratio we would expect for purely transverse magnons which had the same density of states at the transverse (0 MHz) and the longitudinal (ω_n) frequency. However, this may be purely fortuitous, since for the A and D sites of the other alloys there appears to be no systematic trend in the behavior of these relaxation times (see Fig. 9). For the Si sites we see from Table III that T_{01} is usually about a factor of 2 longer than T_{02}. These types of irregular behavior may reflect resonance or virtual magnon states in the spin-wave spectrum.

Wolfram *et al.*[15] have calculated the effects of dilute magnetic impurities on the spin-wave spectrum of an ideal simple-cubic spin-$\frac{1}{2}$ Heisenberg ferromagnet. They find that for a small ratio of impurity-host to host-host exchange, virtual spin-wave states occur which give rise to a large density of states at low energies in the spin-wave spectrum. At low energies the states may be quite narrow. Although these calculations do not apply directly here (i.e., here the interaction between spins is through the conduction electrons[4] and we have a nondilute, spin 0, $\sim\frac{1}{2}$, and ~ 1 system), the phenomenology may be similar.

IV. CONCLUSIONS

The behavior of the enhancement-factor and relaxation-times curves is well described by the drumhead model. Using the drumhead model for the domain wall the enhancement-factor magnitudes and behavior are derived from the equation of motion. The eddy-current damping appears to determine the magnitude of the domain-wall motion and thus the enhancement-factor behavior in pure Fe, whereas because of the increased resistivity and decreased saturation magnetization the stiffness and damping effects appear to be comparable in the ordered alloys. The maximum enhancement factor is found to vary in the same manner as the initial permeability with alloying.

The nuclear relaxation appears to be via emission or absorption of a single bulk magnon, as was found to be the case in pure Fe. The relaxation times vary as much as a factor of 3 or 4 for different sites in the same alloy. This may reflect resonance or virtual magnon levels in the spin-wave spectrum.

[1]M. B. Stearns, Phys. Rev. 129, 1136 (1963).

[2]J. I. Budnick, S. Skalski, and T. J. Burch, J. Appl. Phys. 38, 1137 (1967).

[3]M. B. Stearns, L. A. Feldkamp, and J. F. Ullrich, Phys. Letters 30A, 443 (1969).

[4]M. B. Stearns, this issue, Phys. Rev. B 4, 4069 (1971).

[5]M. B. Stearns, Phys. Rev. 162, 496 (1967).

[6]M. B. Stearns, Phys. Rev. 187, 648 (1969). Equation (4) is printed incorrectly; the exponential should be $e^{-2t(\mathrm{sech}^2 x)/T_{02}}$. However in evaluations of T_{02} the correct form was used.

[7]C. Kittel and J. G. Galt, in *Solid State Physics*, edited by F. Seitz and D. Turnbull (Academic, New York, 1956), Vol. 3, p. 437. Referred to as KG. See also M. Matsuura, H. Yasuoka, A. Hirai, and T. Hashi, J. Phys. Soc. Japan 17, 1147 (1962).

[8]A. C. Gossard, A. M. Portis, M. Rubinstein, and R. H. Lundquist, Phys. Rev. 138, A1415 (1965).

[9]K. H. Stewart, *Ferromagnetic Domains* (Cambridge U.P., Cambridge, England, 1954).

[10]F. W. Glaser and W. Ivanick, Trans. AIME 206, 1290 (1956).

[11]H. Matsumoto, 385th Report, Research Institute for Iron, Steel, and Other Metals, 1936 (unpublished).

[12]M. Fallot, Ann. Phys. 6, 305 (1936).

[13]J. R. Asik and M. B. Stearns, Bull. Am. Phys. Soc. 16, 403 (1971).

[14]T. Moriya, J. Phys. Soc. Japan 19, 681 (1964); R. E. Walstedt, V. Jaccarino, and N. Kaplan, *ibid.* 21, 1843 (1966).

[15]T. Wolfram and J. Callaway, Phys. Rev. 130, 2207 (1963); T. Wolfram and W. Hall, *ibid.* 143, 284 (1966); T. Wolfram, *ibid.* 182, 573 (1969).

PHYSICAL REVIEW B VOLUME 4, NUMBER 11 1 DECEMBER 1971

Luminescence of Neodymium in Barium Magnesium Germanate Crystals and Glass Hosts

Mohan Munasinghe* and Arthur Linz

Center for Materials Science and Engineering, and Department of Electrical Engineering, Massachusetts Institute of Technology, Cambridge, Massachusetts 02139

(Received 17 June 1971)

The optical properties of the rare-earth dopant neodynium in crystal and glass hosts of the identical chemical composition $Ba_2MgGe_2O_7$ have been studied on a comparative basis. This technique offers many advantages. Concentration quenching of emission is seen to commence at <1.0 at.% Nd^{3+} doping in the glass, but not at all for Nd^{3+} concentrations of up to ~2 at.% in the crystal. This and other related concentration- and temperature-dependent phenomena, including multiple-lifetime effects observed in the glass, are shown to be consistent with the existence of two predominant types of resonant-energy-transfer mechanisms between Nd^{3+} ions.

INTRODUCTION

In recent years stimulated emission has been reported in many solid-state hosts doped with various rare-earth ions.[1-3] In this group of activators, Nd^{3+} has been the most extensively used one. In this paper we present the results of an investigation of Nd^{3+} luminescence in crystal and glass hosts of identical chemical composition $Ba_2MgGe_2O_7$.

EXPERIMENTAL DETAILS

All the single crystals of $Ba_2MgGe_2O_7$ were grown by a top-seeded-solution technique.[4] Glass samples were prepared by melting down a stoichiometric mixture of the required chemical composition and cooling it rapidly through the nucleation temperature.[5] All samples were cut and polished to the same dimensions (approximately 5×6×7 mm).